ISBN: 978-3-95450-247-9 ISSN: 2673-5490 doi: 10.18429/JACoW-IPAC2024-WEPC58

MONTE-CARLO PHOTOEMISSION MODEL FOR THIN FILM SEMICONDUCTORS UNDER HIGH FIELDS

C.-K. Huang*, D. A. Dimitrov, A. Alexander, G. Wang, D. Perez, S. Bagchi,
R. Shinohara, E. I. Simakov
Los Alamos National Laboratory, Los Alamos, NM, USA

Abstract

Monte-Carlo models have been successfully used to model bulk semiconductor photocathodes, such as Gallium Arsenide (GaAs) and others. Here we present a Monte-Carlo model under development for the photoemission from semiconductor thin films, such as Cs_2Te, under high acceleration field gradient. Thin films and heterostructures, as well as high photocathode gun operating gradient and cryo-cooling, are both beneficial to high brightness electron sources. Our model employs electronic, phonon, dielectric and optical properties from Density Functional Theory (DFT) calculation and available experimental measurements. Furthermore, a photo excitation model based on the light interference effect in thin films is also being implemented, where our previous work indicates that such effect plays an important role in the photoemission from semiconductor thin films. Preliminary study of the effects of high field gradient on the electron transport is discussed. This Monte-Carlo model will be used to investigate the quality of the emitted electron beams from semiconductor thin films for the cathode development in the CARIE project at LANL and to inform theoretical transport models based on the moment method.

INTRODUCTION

Monte-Carlo method is a powerful technique for modeling semi-classical charge carrier transport in semiconductors in different structures and under various conditions (e.g., with cryocooling or spin transport). For photocathodes, it has been applied to the study of several common cathode materials, such as GaAs, diamond, cesium antimonide (Cs_3Sb) and bialkali antimonide (K_2CsSb).

Cesium telluride (Cs_2Te) is also a desirable semiconductor material for high brightness photocathode due to its relatively large band gap and small electronic affinity. Quantum Efficiency (QE) > 10 % can be reliably achieved, e.g., at 261 (nm), in Cs_2Te thin film photocathode, while Cs_2Te's wide band gap also offers resilience to high gradient operation.

Depending on the details of Monte-Carlo model, simulation of photoemission from semiconductor cathode needs parametrization of the material's bulk, electronic, phonon and surface properties. For Cs_2Te, these parameters, typically from measurements or simple model calibrated with experiment results, are scarce. Therefore, early Monte-Carlo simulation of Cs_2Te photoemission [1] employs reduced transport process similar to those in 3-step theoretical models. More recently, first-principle calculation from DFT [2,3] provide more detailed input to the Monte-Carlo simulation. However, important material properties of Cs_2Te are still in investigation both in theory and experiment. We have conducted first-principles study of Cs_2Te using DFT for its structural, elastic, electronic, and transport properties [4] and are in the process to adopt these results in our Monte-Carlo simulation for Cs_2Te thin film photocathode. The current implementation of our Monte-Carlo model, as well as a theoretical moments model [5] used for comparison, are described. Preliminary results from this Monte-Carlo model are also presented.

* huangck@lanl.gov

PHOTOEMISSION MODEL

Photoemission from semiconductor is commonly modeled as a 3-step process due to Spicer, i.e., photoexcitation, transport and emission. We adopt this 3-step process in both our moments model and the Monte-Carlo model.

Photoexcitation in Thin Film Cathode

The photon absorption process occurs within tens of nm in a thin film Cs_2Te photocathode, therefore, light absorption profile plays a role in photoexcitation for relatively thin films with thickness comparable to the photon absorption depth. Furthermore, for Cs_2Te thin film grown on a substrate, such as Mo, light transmission and reflection may also change the intensity profile within the photocathode layer. Similar to other work, we assume one electron is excited for each absorbed photon. The light interference effect is accounted for through the modified rate of light absorption profile proportional to $|E_{ph}(x)|^2$ assuming plane wave of amplitude E_0 in normal incidence, where the exact solution is

$$E_{ph}(x) = E_0(t_1 e^{ik_1 x} + r_1 e^{-ik_1 x}). \tag{1}$$

t_1 and r_1 for a cathode with thickness L are given in [6],

$$\begin{aligned}
\begin{bmatrix} t_1 \\ r_1 \end{bmatrix} &= \frac{1}{2n_1}\begin{bmatrix} (n_1+n_0)+(n_1-n_0)r_0 \\ (n_1-n_0)+(n_1+n_0)r_0 \end{bmatrix}, \\
r_0 &= \frac{B+A}{(n_0+n_1)/(n_0-n_1)B + (n_0-n_1)/(n_0+n_1)A}, \\
A &= (n_1-n_2)(n_0+n_1)e^{ik_1L}, \\
B &= (n_1+n_2)(n_0-n_1)e^{-ik_1L},
\end{aligned} \tag{2}$$

where n_0, n_1 and n_2 are the complex refractive indexes of vacuum, cathode and substrate, respectively. We use $n_1(\omega)$ from DFT calculation of the bulk optical properties, e.g., $n_1 \approx 1.566 + 1.318i$ for $\lambda = 261$ nm ($\hbar\omega = 4.75$ eV), and $n_2 = 0.6467 + 3.0555i$ for Mo.

ISBN: 978-3-95450-247-9 ISSN: 2673-5490 doi: 10.18429/JACoW-IPAC2024-WEPC58

From this solution, $R(\omega)$ and $T(\omega)$, i.e., the transmission and reflection coefficients of the photocathode layer in between the vacuum and substrate for photon of energy $\hbar\omega$ can be calculated. Then, $A(\omega) = 1 - R(\omega) - T(\omega)$ is the fraction of laser energy absorbed.

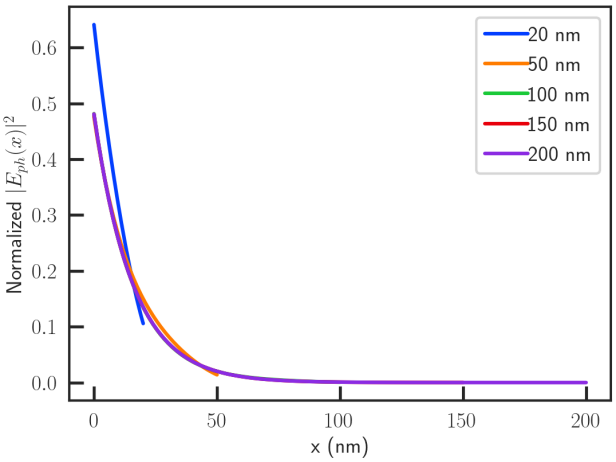

Figure 1: Normalized $|E_{ph}(x)|^2$ profile within Cs_2Te cathode for various thicknesses. Laser wavelength is $\lambda = 261$ nm.

Figure 1 shows the normalized $|E_{ph}(x)|^2$ profiles in a Cs_2Te cathode on Mo substrate for various cathode thickness and a laser light of wavelength $\lambda = 261$ nm. We note that these profiles can be reasonably fitted as exponential functions of the form e^{a-bx}. Defining $\tilde{x} \equiv x/L$, we have the following fit for $\lambda = 261$ nm,

$$ln(|E_{ph}(\tilde{x})|^2) = a - b\tilde{x} \approx -3.11\times10^{-7}L^3 + 1.27\times10^{-4}L^2 - 1.65\times10^{-2}L - 0.0685 + \tilde{x}\times(8.91\times10^{-10}L^4 + 5.49\times10^{-8}L^3 - 1.25\times10^{-4}L^2 - 0.0431L - 0.831). \quad (3)$$

This approximation has $< 5\,\%$ error for most of the range of cathode thickness $L < 200$ nm and location inside the layer, with maximum error of about 20 % only for $L < 50$ nm and $x/L < 0.2$. For $L = 200$ nm, this indicates that the photon absorption length is $\delta \approx 16$ nm, while for $L = 20$ nm, $\delta \approx 11.5$ nm.

Figure 2 shows the photon absorption fraction $A(\omega)$ for Cs_2Te cathode on Mo substrate when the cathode thickness L is varied. The absorption increases quickly with L for very thin cathode. It is maximized for $L \approx 32$ nm, then drops toward the bulk cathode limit when L is further increased.

The above approximation of the modified rate of light absorption profile is used to initialize the initial locations of electrons inside the cathode for subsequent transport calculation. The energy of the electron is uniformly sampled from $E_a < E < (\hbar\omega - E_g)$, where E_a and E_g are electron affinity and band gap of Cs_2Te. The initial electron distribution is isotropic and placed in the lowest conduction band.

Electron Transport and Emission

Our Monte-Carlo transport model is similar to the one in [1]. But instead of assuming a mean scattering energy

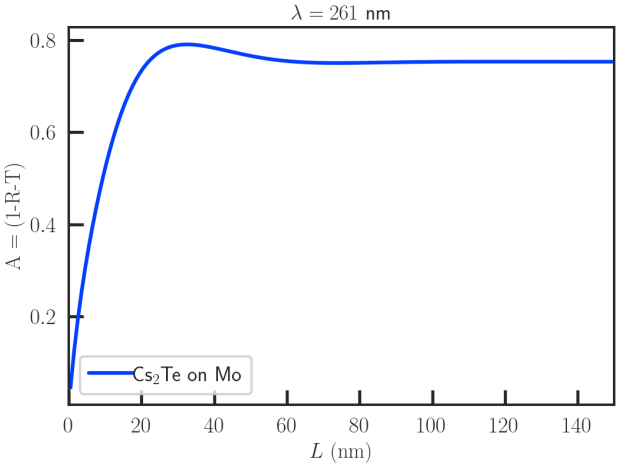

Figure 2: Photon absorption fraction as function of Cs_2Te cathode thickness.

Table 1: Parameters for the Cs_2Te Transport Simulation

Parameter	Value
Photon energy $\hbar\omega$	4.75 eV
Band gap E_g	3.3 eV [7]
Γ_1 valley effective mass (m_1^*)	0.27 m_0
Γ_2 valley effective mass (m_2^*)	0.7 m_0
$\Gamma_1 - \Gamma_2$ splitting energy E_s	0.796 eV
Phonon energy E_{ph} (estimate)	0.01 eV
Deformation constant D_i (estimate)	10^{11} eV/m
Dielectric constant ϵ_s	10.3 ϵ_0
High frequency dielectric constant ϵ_∞	4.3 ϵ_0
Density ρ	3.99 g/cm^3
Temperature T	300 K
Electron affinity E_a	0.25 eV

loss of 5 meV and an energy independent electron mean free path of 3 nm, we include in the transport the dominant scattering processes, i.e., polar optical phonon and intervalley scatterings consistent with recent modeling effort, and the effect of the second conduction band [8]. The parameters of the transport simulation are taken from DFT calculation or simple estimate, as well as experimental value when available (see Table 1). m_0, ϵ_0 are electron mass and vacuum permittivity, respectively. For the dielectric constants, we average the corresponding dielectric tensors over three directions. We have also computed the phonon scattering rate directly from DFT, which can be used in the Monte-Carlo simulation for more accurate modeling. Currently a simple electron escape model like [1] is used for emission, i.e, electron is tallied when it reaches the cathode-vacuum interface and its longitudinal energy is large than E_a. Otherwise it is reflected back into the cathode.

It is common to model the electron transport process using its probability to reach the emission surface. The probability for an electron to travel a distance d without scattering is $P(\lambda_{mfp}) = e^{-d/\lambda_{mfp}}$, where $\lambda_{mfp}(E)$ is the mean free path of an electron of energy E. Thus, for an electron initially at distance x from the surface and moving at an angle θ

ISBN: 978-3-95450-247-9 ISSN: 2673-5490 doi: 10.18429/JACoW-IPAC2024-WEPC58

relative to the surface normal, the probability to reach the surface is $P(x, \lambda_{mfp}, \theta) = e^{-x/(\lambda_{mfp}\cos\theta)}$. In [5], $\lambda_{mfp}(E)$ is determined by the polar optical phonon scattering process and is significantly higher than 3 nm when electrons have large energies in the conduction band. Figure 3 shows that for $E > E_a$, this $\lambda_{mfp}(E)$ can be reasonably fitted with a power law E^{β} with $\beta \approx 0.74$.

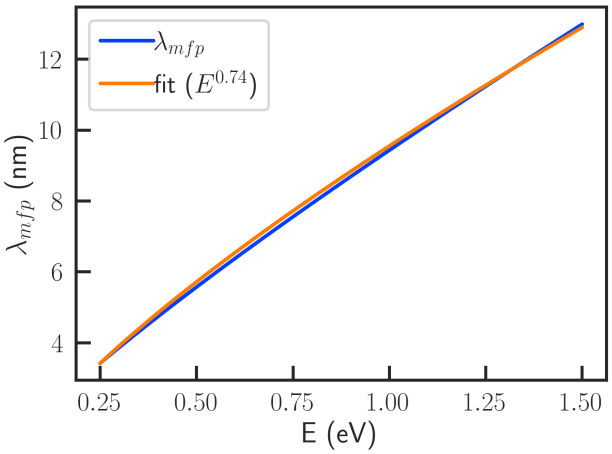

Figure 3: Electron mean free path in Cs_2Te cathode due to polar optical phonon scattering.

With the above approximations, the moments model for the quantum efficiency [5] without applied electric field can be written as,

$$QE = A(\omega)\frac{\int_{E_a}^{\hbar\omega-E_g} dEE \int_{\sqrt{E_a/E}}^{1} duD(Eu^2)uf}{2\int_{E_a}^{\hbar\omega-E_g} dEE \int_{\sqrt{E_a/E}}^{1} du}, \quad (4)$$

where $u = \cos\theta$, $D(y) = H(y - E_a)$, and $f = e^{a}\lambda_E u\left(1 - e^{-L/\lambda_E u - b}\right)/(b\lambda_E u/L + 1)$. $H(y)$ is the Heaviside function, and $\lambda_E = \lambda_{mfp}(E_a)E^{\beta}$.

Simulation Result

To illustrate the effects on the electron transport from cathode thickness and external field, Monte-Carlo simulations are conducted with the photon absorption fraction set to unity. The enhancement of QE is shown in Fig. 4. The transport is enhanced by about 7 % when the cathode thickness is reduced from 200 nm to 20 nm. For an external electric field of 50 MV/m, the transport itself is enhanced by about 27 % and becomes almost independent of the cathode thickness. We note that in this case, QE dependence on the thickness is primarily due to the photon absorption (Fig. 2).

SUMMARY

A Monte-Carlo photoemission model for thin film semiconductor photocathode that takes into account of optical interference effect, detailed transport processes and material properties calculated by DFT is presented. This model is applied to Cs_2Te to show the enhancement of the transport due to thickness and external electric field. This model can be used to improve other 3-step models and for experiment validation.

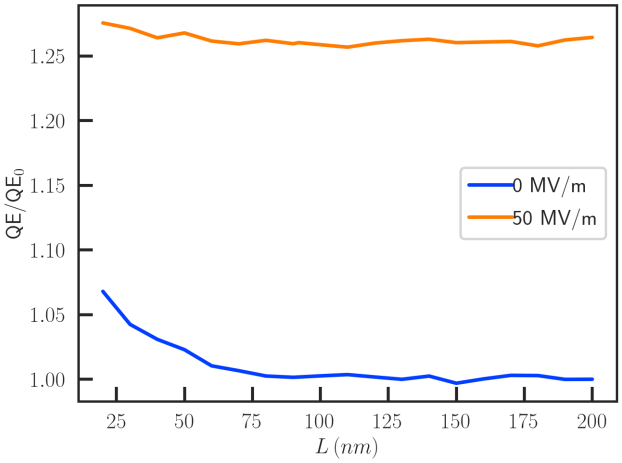

Figure 4: Enhancement of the electron transport due to cathode thickness and external field. QE is calculated for $A(\omega) = 1$ and $\lambda = 261$ nm. QE_0 is defined for the case $L = 200$ nm and no electric field is applied.

ACKNOWLEDGEMENTS

Work supported by the Laboratory Directed Research and Development program of Los Alamos National Laboratory, under project number 20230011DR. This research used resources provided by the Los Alamos National Laboratory Institutional Computing Program, which is supported by the U.S. Department of Energy National Nuclear Security Administration under Contract No. 89233218CNA000001.

REFERENCES

[1] G. Ferrini, P. Michelato, and F. Parmigiani, "A Monte Carlo simulation of low energy photoelectron scattering in Cs_2Te," *Solid State Commun.*, vol. 106, no. 1, pp. 21, 1998. doi:10.1016/S0038-1098(97)10237-X

[2] C. M. Pierce, J. K. Bae, A. Galdi *et al.*, "Beam brightness from Cs–Te near the photoemission threshold," *Appl. Phys. Lett.*, vol. 118, no. 12, p. 124101, 2021. doi:10.1063/5.0044917

[3] C. Cocchi, H. Saßnick, "Ab initio quantum–mechanical predictions of semiconducting photocathode materials," *Micromachines*, vol. 12, pp. 22-24, 2021. doi:10.3390/mi12091002

[4] G. Wang, J. Zhang, C.-K. Huang, D. A. Dimitrov, A. M. Alexander, and E. I. Simakov, "A first-principles study of structural, elastic, electronic, and transport properties of Cs_2Te," 2024. doi:10.48550/arXiv:2405.04398

[5] D. Dimitrov *et al.*, "Modeling optical interference effects for optimization of electron emission properties from thin film semiconductor photocathodes", in *Proc. IPAC'23*, Venice, Italy, May 2023, pp. 1378–1381. doi:10.18429/JACoW-IPAC2023-TUPA012

[6] K. L. Jensen *et al.*, "An extended moments model of quantum efficiency for metals and semiconductors," *J. Appl. Phys.*, vol. 128, no. 1, p. 015301, Jul. 2020. doi:10.1063/5.0011145

ISBN: 978-3-95450-247-9 ISSN: 2673-5490 doi: 10.18429/JACoW-IPAC2024-WEPC58

[7] R. Powell *et al.*, "Photoemission Studies of Cesium Telluride," *Phys. Rev. B*, vol. 8, pp. 3987-3995, 1973. doi:10.1103/PhysRevB.8.3987

[8] C. Huang *et al.*, "Transport model and Monte-Carlo simulations for photoemission from thin film semiconductors under high fields", in *Proc. IPAC'23*, Venice, Italy, May 2023, pp. 1382–1385. doi:10.18429/JACoW-IPAC2023-TUPA014